

Model-Based Analysis of Corrosion Test Results and Extraction of Long-Term Corrosion Rates

N. Li¹, J. S. Zhang¹, H. D. Yu¹, and J. Jansen²

¹Los Alamos National Laboratory

²Idaho National Laboratory

September 22, 2006

This report presents the status of the model-based analysis of the publicly reported corrosion test data and use of the model to extract long term corrosion rates, a main analytical task of the LANL’s Gen IV LFR Work Package “Lead Coolant Testing”. It includes a brief overview of the framework for modeling system corrosion kinetics of steels in oxygen controlled lead and lead-alloys and key results, sources and categories of test data (with the attachment of an electronic database to be submitted separately due to its large size), and analysis results. For the test results of steels in a number of LBE (and Pb) loops, we used our oxidation and corrosion kinetic model to scale the majority of the data into one universal curve, and the scales in length and time determine the asymptotic thickness of the oxides and the liquid metal corrosion rates. These results cannot be obtained from any other previous models and the typical measurements applied to the tested specimens, since some important mechanisms were missing and key aspects of the tests difficult to measure directly.

Based on the current available data, we find that a limited number of steels tested (e.g. EP823) have the requisite long-term corrosion rates for applications at 550°C for more than a few years. Many other materials (e.g. HT-9, T91, 316L) can be used for short to medium terms, or at lower temperatures, or in thick components and structures. However, their larger than 10 microns/year corrosion rates make them unsuitable for fuel cladding in 10-30 years long-life cores at 550°C in the as available compositions and forms. Similar conclusion may be inferred from very limited test results for steels in Pb, which showed no substantial difference in terms of corrosion resistance from that in LBE. Since results are very scarce for tests longer than 3000 hrs, and the corrosion rates also depend on test loop flow and temperature distributions that are usually not well reported, there are still significant uncertainties in the conclusions and predictions.

Longer-term tests are beginning to be performed, and some promising alloy modifications (e.g. Si or Al enhancement) and/or surface treatments (e.g. functionally graded materials) are being developed and tested. Since the required corrosion resistance is already achieved for short to medium term uses, and are within reach for the expected long-term applications, we believe a level of materials development and test efforts should be sustained, and it is possible to proceed to the next level of reactor development (e.g. engineering scale test and demonstration, and design of test and demonstration reactors with LBE coolant at medium temperatures with replaceable cores).

Overall, our compilation of the wide ranging test data and the systematic model-based analysis result in a substantially higher level of understanding of steel corrosion in heavy liquid metal systems, and should provide good guidance for further development and

testing, and reliable framework to interpret the results and predict long-term corrosion rates.

Modeling System Corrosion Kinetics

With support from the DOE AFCE, LANL initiated a sustained effort to establish a system kinetic model of corrosion in oxygen controlled LBE/Pb and has gradually incorporated the key processes and mechanisms of surface oxidation, scale removal by flow liquid metal, mass transfer and deposition of corrosion products.

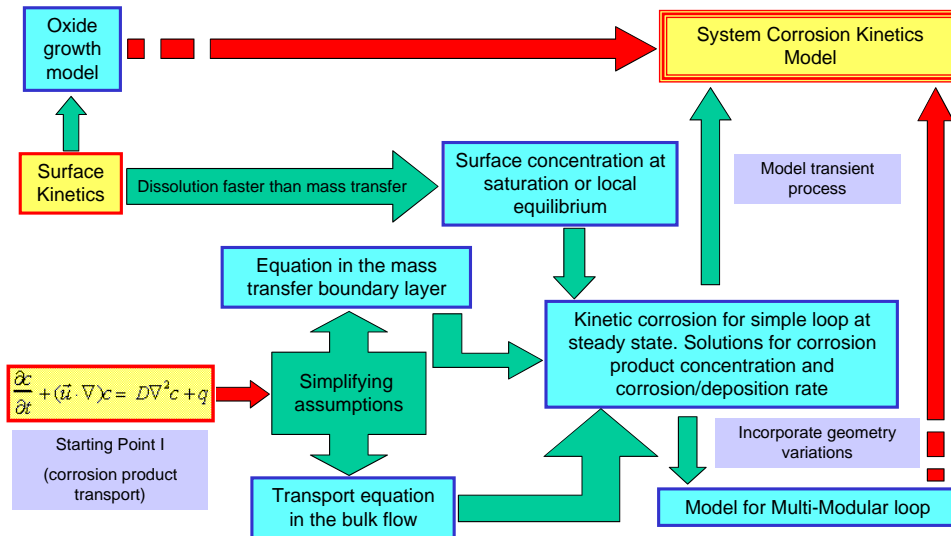


Figure 1. Framework of modeling system corrosion kinetics in closed flowing systems.

This model is more complete in its direct coupling of hydrodynamics to surface reactions, has higher fidelity than the existing local and sectioned models, and has been benchmarked successfully against a number of liquid metal loop test experiments. In particular, we clearly identified and modeled the scale removal of oxidized steels in oxygen controlled lead and lead-bismuth eutectic, and can use the model to extract long-term corrosion rates from measured oxide thickness in short times. The long-term corrosion rates have not been directly measured by most experimental groups, or reported in their analyses. For Gen IV LFR, however, long-term corrosion rates are critical for long-life core designs. Some key results of the modeling are summarized below.

First, the kinetic modeling of mass transfer processes in flowing liquid metal in non-isothermal loops successfully captured the effects of oxygen concentration, the non-uniform distribution of corrosion and deposition (e.g., the “down-stream” effects), and the transient to steady state and the effects of corrosion product build-up in closed loops. In test loops (and by extension technological systems) built with materials of similar corrosion resistance to the test materials, this finding cautions the use of loop-test data:

- The corrosion rate depends on the global (loop) conditions (temperature and flow distribution). So using local conditions to describe corrosion can lead to grossly inaccurate conclusion. For instance, corrosion rate can vary substantially in an isothermal section of a non-isothermal test loop, and the rate measured at some intermediate temperature locations (a typical use of loops to measure corrosion at different temperatures) can be quantitatively or even qualitatively different from that at the same temperature but in a different configuration.
- In static testing, due to limited mass transfer in the liquid metals, and the changing corrosion product concentration, long-term corrosion may not be measured at all (see discussions next).

Second, after incorporating the effects of oxide growth and corrosion through the protective oxides, the corrosion can be modeled as the composite of two processes: oxidation of steels (following a predominantly parabolic law) and scale removal through the oxides (linear in time, where the rate depends on global conditions). In a simplified version (not considering alloy composition effects and spatially heterogeneous effects), the observed/measurable effects are:

- The oxide thickness grows parabolically in the early time, while the rate constant may be computed based on Wagner's theory.
- The scale removal effect begins to manifest most prominently in the weight changes of the materials: weight increase due to oxidation peaks in relatively short time (a few hundred hours at 500°C with LBE flowing at 2m/s), then starts to decrease, eventually approaching the long-term corrosion rate (in longer than several thousand hours under the aforementioned conditions). The effect on oxide thickness is little in the same time period.
- Over the long run, the oxide growth will be balanced by the scale removal and approach a limiting thickness. If the oxide stays structurally stable (against spallation), then a constant long-term corrosion rate may be attained.
- Static testing cannot measure long-term corrosion rate in flowing HLMC systems. However, due to the ease of such testing, it is very valuable as a means to screen materials with suitable oxide growth and stability, and protective coatings.

Applying the observations above to the majority of the reported corrosion data, we conclude that the measured thickness of oxidation, while an important factor for the short- to medium-term corrosion behavior, is not directly related to the long-term corrosion rate. It is possible to extract the long-term corrosion if the oxide thickness is carefully measured, as demonstrated below.

Generally, high-temperature oxidation with scale removal simultaneously involves both thermodynamics and kinetics. Because of the fast oxidation reaction, the process reaches local thermodynamic equilibrium quickly. Kinetics, such as species diffusion, becomes the most important and dominates. In the temperature range of interest, the kinetics can be described by a parabolic rate constant for oxidation, K_p , and a linear rate constant for scale removal, K_r . The oxide thickness, x , observes Tedmon's equation:

$$\frac{dx}{dt} = \frac{K_p}{2x} - K_r. \quad (1)$$

The solution for $x(t=0) = 0$ (no pre-oxidation) is:

$$t = -\frac{x}{K_r} - \frac{K_p}{2K_r^2} \ln \left| 1 - \frac{2K_r}{K_p} x \right|. \quad (2)$$

Eq.(1) is demarcated by $x < x_f$ for oxide growth and $x > x_f$ for oxide thinning, where

$$x_f = \frac{K_p}{2K_r}. \quad (3)$$

It is clear that x_f is the asymptotic oxide thickness, assuming it is structurally stable (no spalling). The oxide thickness and time can then be scaled as

$$X = \frac{x}{x_f} = \frac{2K_r x}{K_p}, \quad \tau = \frac{t}{t_c} = \frac{2K_r^2 t}{K_p}, \quad (4)$$

where $t_c = K_p / 2K_r^2 = x_f / K_r$ is not the time for achieving the asymptotic thickness. It is twice the time needed to reach the asymptotic oxide thickness following a pure parabolic growth law. Eq.(2) becomes:

$$\tau = -X - \ln|1 - X|. \quad (5)$$

In this work, we perform weighted nonlinear fitting using Eq. (2) to obtain K_p and K_r for all steels in each loop. The weighting factor is determined by $w_i = x_i / x_{max}$ for the i th data point, $i=1,2,\dots,n$. w_0 is set 1. The universal scalings are analyzed through Eq. (4).

Sources and Categories of Test Results

Corrosion tests of a wide variety of materials under wide ranging conditions have been carried out in both static (in crucibles) and dynamic (in isothermal or non-isothermal flow loops) LBE/Pb environments. The steels tested include ferritic and martensitic steels (P22, F82H, STBA28, T91, NF616, ODS-M, Eurofer 97, STBA26, Optifer IVc, EM10, Manet II, 56T5, ODS, EP823, HT9, HCM12A, HCM12, 410ss, T410, 430ss, etc.), and austenitic steels (D9, 14Cr-16Ni-2Mo, 1.4970, 316L, 304L, 1.4984, etc.). The test temperatures range from 300 – 650°C, times from 100 – 10,000 hours (tests longer than 3000 hrs are mostly in static LBE/Pb). The oxygen concentrations vary from depleted (10^{-12} wt%) to saturated ($\sim 10^{-4}$ wt%). The range covers the oxygen control band that is below the formation of PbO and above the formation of Fe₃O₄, which is temperature dependent. The following is a tally of the test results available as of fall, 2005 that we collected:

- There are over 22 ferritic/martensitic steels (including a number of ODS steels), and 6 austenitic steels tested in stagnant and/or flowing LBE and/or Pb. The test duration ranges from a few hundred hours to up to 10000 hrs (the longer durations are mostly for stagnant testing).

- In stagnant LBE (in crucibles, with or without oxygen control), more than 165 results for F/M steels and over 102 for austenitic steels are available.
- In flowing LBE (in loops, usually with oxygen control), more than 70 results for F/M steels and over 42 for austenitic steels are reported.
- In Pb, 12 results are reported for stagnant testing, while 20 are reported for dynamic (flowing) testing.
- Most groups only analyzed oxide growth based on simple oxidation power laws, and were not able to extract liquid metal corrosion rates. This is complicated by the difficulty in measuring weight changes due to residual LBE/Pb on specimens.

The general conclusions may be drawn as the following:

- For unprotected steels (no coatings), the necessity and efficacy of oxygen control are validated in all tests, i.e. in-situ growth of surface oxide layers on steels in LBE/Pb with sufficient concentration of oxygen significantly reduces corrosion.
- In static tests within the oxygen control band, most martensitic and austenitic steels form oxides that are protective under $\sim 550^{\circ}\text{C}$, especially for oxygen concentrations above 10^{-6} wt%.
- In dynamic tests, most of which are in LBE and the oxygen concentrations are in 10^{-6} - 10^{-5} wt% range, the austenitic and martensitic steels formed protective oxides.
- Between 550 - 600°C , the formation and protectiveness of oxides on martensitic steels are uncertain for durations up to a few hundred hours, but usually fail after that. For austenitic steels, the oxides are thin and not completely protective at $\sim 550^{\circ}\text{C}$.

Steels	Stagnant LBE	Flowing LBE	Stagnant Pb	Flowing Pb
(I) Austenitic: 316L, 304L, D9, 1.4948, 1.4970, 14Cr-16Ni-2Mo	$T = 300\text{-}600^{\circ}\text{C}$, $c_{\text{O}} = 10^{-10}\text{-}c_{\text{O},s}$, $t = 100\text{-}10,000h$	$T = 400\text{-}600^{\circ}\text{C}$, $c_{\text{O}} = 10^{-9}\text{-}10^{-5}$, $t = 133\text{-}10,000h$ (mostly 316L)	$T = 550, 464^{\circ}\text{C}$, $c_{\text{O}} = 8 \times 10^{-6}$, $c_{\text{O},s}$, $t = 1,200,$ $3,000h$ (1.4970, 316L)	$T = 400, 500^{\circ}\text{C}$, $c_{\text{O}} = 3\text{-}4 \times 10^{-5}$, $t = 3,027h$ (1.4948, 1.4970)
(I) Ferritic/Martensitic: T91, HT-9, EP823, F82H, Manet II, EM10, Eurofer 91, Optifer IVc, HCM12, HCM12A, T410, 430, 56T5, STBA26, T22, T122, 9Cr-2WVTa	$T = 300\text{-}650^{\circ}\text{C}$, $c_{\text{O}} = 10^{-12}\text{-}c_{\text{O},s}$, $t = 100\text{-}10,000h$ (mostly T91, HT-9, EP823)	$T = 300\text{-}600^{\circ}\text{C}$, $c_{\text{O}} = 10^{-9}\text{-}10^{-5}$, $t = 133\text{-}10,000h$	$T = 464\text{-}550^{\circ}\text{C}$, $c_{\text{O}} = 8 \times 10^{-6}$, $c_{\text{O},s}$, $t = 1,200\text{-}$ $3,700h$ (Optifer IVc, F82H)	$T = 400, 500^{\circ}\text{C}$, $c_{\text{O}} = 3\text{-}4 \times 10^{-5}$, $t = 3,027h$ (Optifer IVc, EM10)
(I.alt) Al-coating: GESA, pack cementation	$T = 350\text{-}650^{\circ}\text{C}$, $c_{\text{O}} = 10^{-10}\text{-}10^{-4}$, $t = 100\text{-}10,000h$	$T = 450\text{-}520^{\circ}\text{C}$, $c_{\text{O}} = 10^{-7}\text{-}10^{-5}$, $t = 133\text{-}400h$		$T = 550^{\circ}\text{C}$, $c_{\text{O}} = 10^{-6}$, $t = 1,500,$ $3,000h$
(I.alt) Surface-treated: shot-peening		$T = 450\text{-}520^{\circ}\text{C}$, $c_{\text{O}} = 10^{-7}\text{-}10^{-5}$, $t = 133\text{-}400h$		
(II) Si modified: 1-5% Si addition in 2-12% Cr alloys, 18Cr-20Ni-5Si	$T = 400\text{-}700^{\circ}\text{C}$, $c_{\text{O}} = c_{\text{O},s}$, $t = 100\text{-}3,000h$	$T = 450\text{-}520^{\circ}\text{C}$, $c_{\text{O}} = 10^{-7}\text{-}10^{-5}$, $t = 133\text{-}400h$		

(II) Oxide Dispersion Strengthened: ODS-M (9Cr-2W), MA957	$T = 500-650^{\circ}C$, $c_{O} = 10^{-6}$, $t = 800-5,000h$	$T = 550^{\circ}C$, $c_{O} = 10^{-7}-10^{-5}$, $t = 2,000-10,000h$		
---	---	--	--	--

Table 1. Reported test conditions and durations for steels in LBE and Pb.

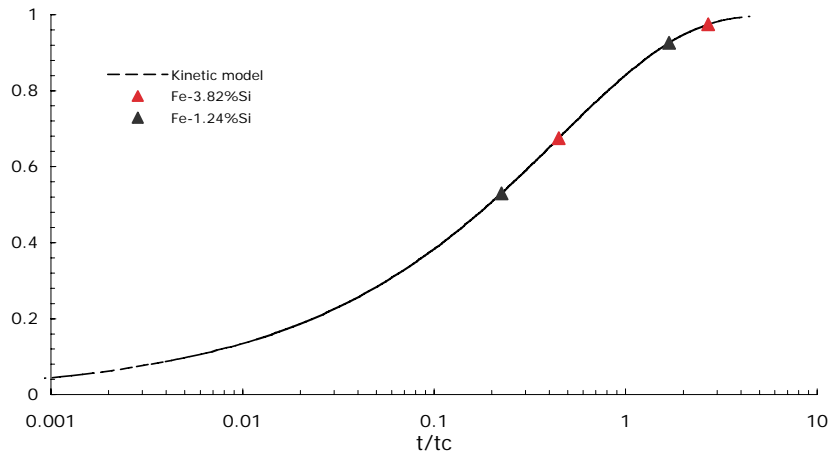
Results

We performed analyses based on our kinetic modeling of the oxidation and corrosion of steels in LBE/Pb. Using several data sets with well defined test conditions in loops, we were able to extract the long-term corrosion rates which have not been reported by the others (very difficult to measure, especially in the short to medium duration tests), and had not been contained in the analyses conducted or models used. These rates are essential for LFR long-life core designs, and the modeling clarifies a complex process that had not been adequately studied and understood. We characterize the temperature, alloy composition dependence, and loop dependence of the oxidation and corrosion rates.

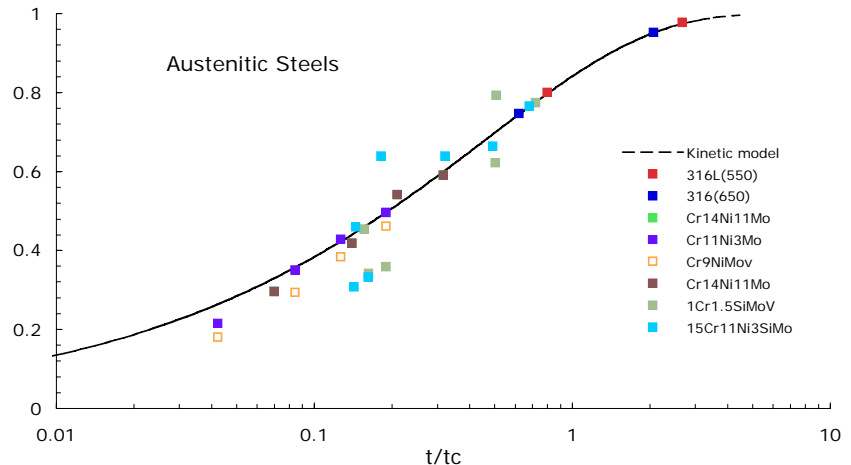
Our analysis of the collected data shows great promise of the model-based approach for analyzing the wide-ranging test results reported by groups from around the world. Our modeling also revealed the inadequacy of tests performed in static and/or low flow environment for extracting long-term corrosion rates, and the difficulty to analyze this class of data (the majority of the reported results).

The key results obtained to-date are as follows:

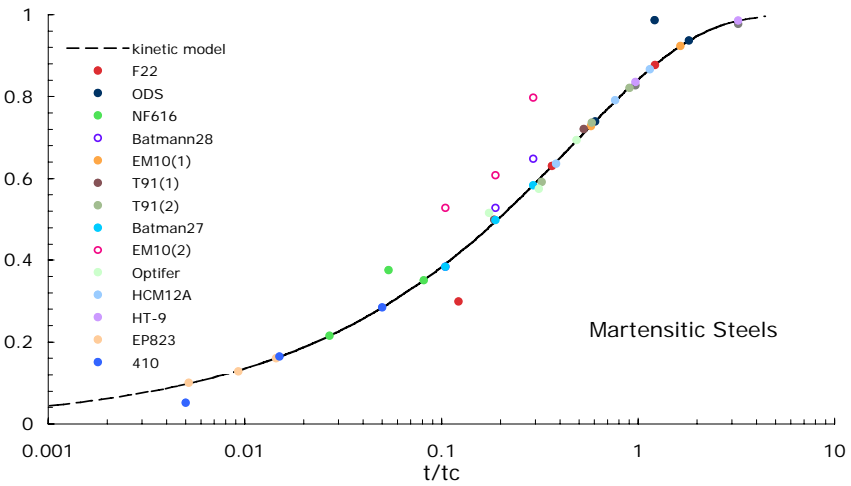
- Compilation of the experimental oxidation/corrosion studies and creation a cohesive database, including references and key graphs and pictures, see attachment.
- Separate analyses of individual steels of loop test data for following LBE and Pb to extract oxidation and corrosion rates, which are highlighted below.



(a)



(b)



(c)

Figure 2. Separate model-based scaling analyses of three different classes of tested materials, (a) Fe-Si alloys; (b) austenitic steels, and (c) ferritic/martensitic steels.

- Tabulate results in the database. To assist the examination of the effects of Cr concentration, temperature, and loop, the same results are organized in three tables below. There are a number of loop test results not included here yet. In addition, we have not included tests from the static tests, since the results are much more difficult to interpret and conditions vary widely.

Cr Composition	Temperature	Material	k_p	k_r	Xf
wt%	°C		m^2/s	micron/yr	micron
Fe-Si					
	700	Fe-3.82%Si	8.97E-17	235.61	6.00
		Fe-1.24%Si	3.82E-17	108.89	5.53
Martensitic steel (Ni<1%)	Ni<1%				
2.139	550	F22	5.54E-16	305.24	28.63
8.67	530	ODS	1.92E-16	283.67	10.69

8.82	530	NF616	5.70E-17	32.60	27.57
8.97	470	EM10	8.67E-17	140.17	9.75
8.98	470	T91	9.84E-17	84.77	18.30
8.98	470	T91	5.84E-17	48.36	19.03
9	470	Batman27	3.64E-17	21.73	26.40
9.1	470	Optifer lvc	8.61E-17	43.09	31.52
10.83	530	HCM12A	1.46E-16	196.27	11.7
12	550	HT-9	8.07E-17	189.97	6.70
12	470	EP823	1.00E-17	2.53	62.27
12.5	550	410	1.12E-17	8.81	20.06
Austenitic Steel	Ni>1%				
1	550	1Cr1.5Si-MoV	8.77E-16	78.84	175.42
11	550	Cr11Ni3Mo	6.60E-17	11.33	91.78
14	550	Cr14Ni11Mo	2.30E-17	8.61	42.05
15	550	15Cr11Ni3SiMoNb	2.44E-17	12.78	30.13
16.34	550	316L	2.74E-17	100.49	4.30
16.34	650	316L	1.44E-16	203.09	11.20

(a)

Temperature	Cr Composition	Material	kp	kr	Xf
°C	wt%		m ² /s	micron/yr	micron
Fe-Si					
700		Fe-3.82%Si	8.97E-17	235.61	6.00
		Fe-1.24%Si	3.82E-17	108.89	5.53
Martensitic steel	Ni<1%				
470	8.97	EM10	8.67E-17	140.17	9.75
470	8.98	T91	9.84E-17	84.77	18.30
470	8.98	T91	5.84E-17	48.36	19.03
470	9	Batman27	3.64E-17	21.73	26.40
470	9.1	Optifer lvc	8.61E-17	43.09	31.52
470	12	EP823	1.00E-17	2.53	62.27
530	8.67	ODS	1.92E-16	283.67	10.68
530	8.82	NF616	5.70E-17	32.60	27.57
530	10.83	HCM12A	1.46E-16	196.27	11.7
550	2.139	F22	5.54E-16	305.24	28.63
550	12	HT-9	8.07E-17	189.97	6.70
550	12.5	410	1.12E-17	8.81	20.06
Austenitic Steel	Ni>1%				
550	1	1Cr1.5Si-MoV	8.77E-16	78.84	175.42
550	11	Cr11Ni3Mo	6.60E-17	11.33	91.78
550	14	Cr14Ni11Mo	2.30E-17	8.61	42.05
550	15	15Cr11Ni3SiMoNb	2.44E-17	12.78	30.13
550	16.34	316L	2.74E-17	100.49	4.30
650	16.34	316L	1.44E-16	203.09	11.20

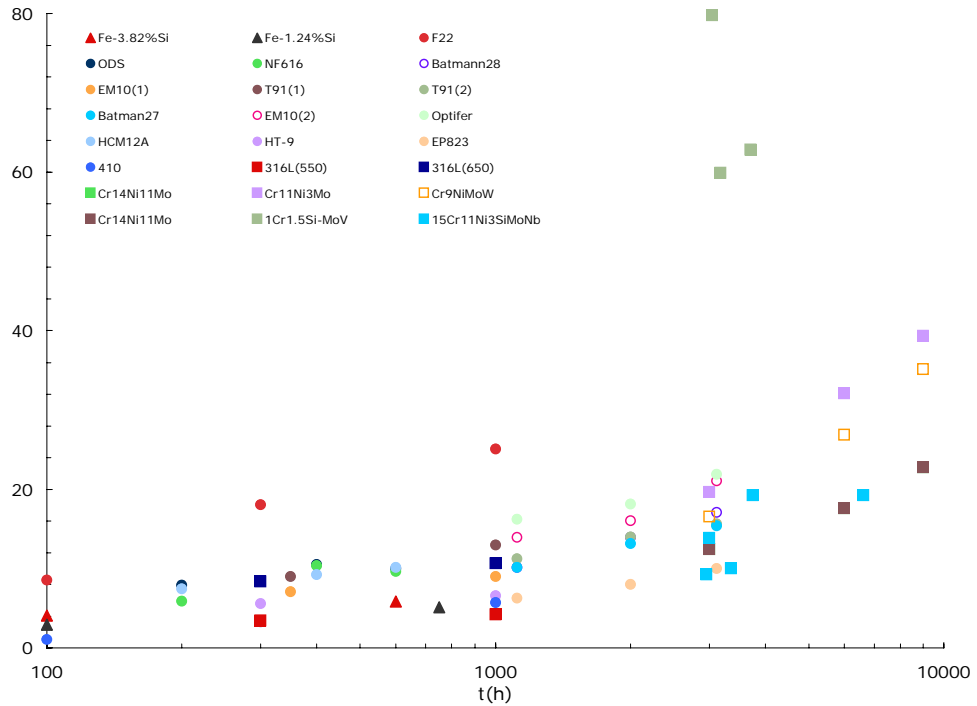
(b)

loop	Temperature	Material	kp	kr	Xf
	°C		m ² /s	micron/yr	micron
Barbier et al (IPPE loop)	470	T91	5.84E-17	48.36	19.03
		Batman27	3.64E-17	21.73	26.40
		Optifer lvc	8.61E-17	43.09	31.52
		EP823	1.00E-17	2.53	62.27
Balbaud et al (IPPE loop)	470	EM10	8.67E-17	140.17	9.75
		T91	9.84E-17	84.77	18.30
Machut (LANL DELTA)	530	ODS	1.92E-16	283.67	10.69
		NF616	5.70E-17	32.60	27.57
		HCM12A	1.46E-16	196.27	11.7
Loewen et al (INL, not a true loop)	550	F22	5.54E-16	305.24	28.63
		HT-9	8.07E-17	189.97	6.70
		410	1.12E-17	8.81	20.06
		316L	2.74E-17	100.49	4.30
	650	316L	1.44E-16	203.09	11.20
	700	Fe-3.82%Si	8.97E-17	235.61	6.00
		Fe-1.24%Si	3.82E-17	108.89	5.53
Adamov et al (unspecified Pb loop)	550	Cr11Ni3Mo	6.60E-17	11.33	91.78
		Cr14Ni11Mo	2.30E-17	8.61	42.05
Gorynin et al (IPPE loops)	550	1Cr1.5Si-MoV	8.77E-16	78.84	175.42
		15Cr11Ni3SiMoNb	2.44E-17	12.78	30.13

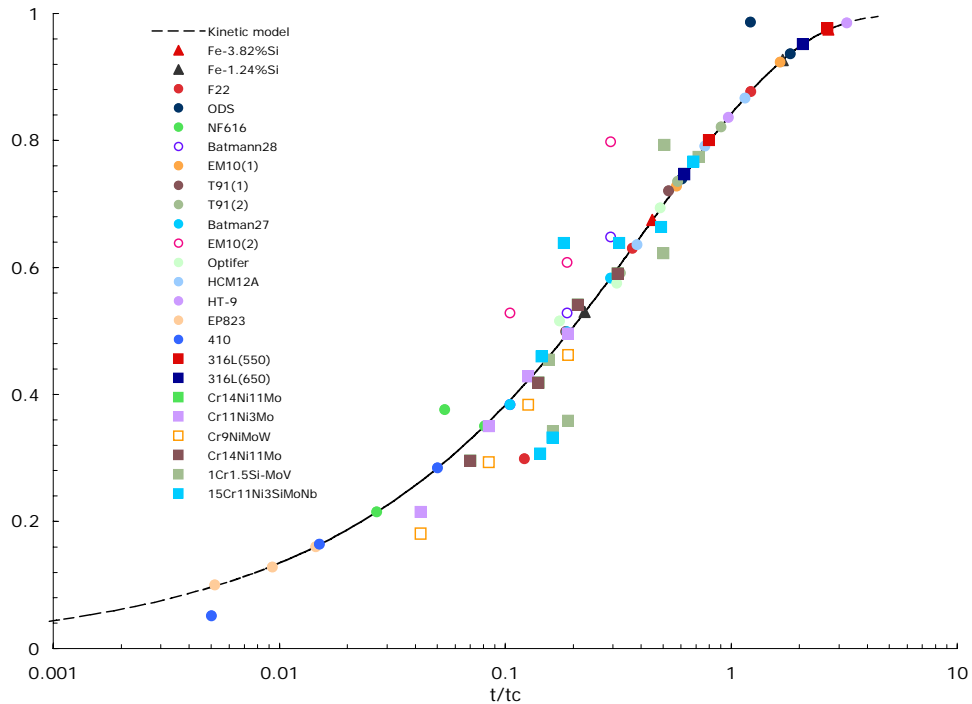
(c)

Table 2. The asymptotic thickness of the protective oxides and the liquid metal corrosion rates for a number of steels tested in LBE loops, in (a) ascending Cr concentrations, (b) increasing temperatures, and (c) different test loops.

- Universal scaling of data sets. Based on the results from nonlinear least square fitting of the test results to the model, we have collapsed the majority of the data points onto one universal curve. While there are still scatters, the general trend becomes very clear. The mostly commonly used power-law (usually parabolic) growth of oxides cannot be applied here, and completely masked the contributions from liquid metal corrosion. A paper is in preparation for submission to an archival journal.



(a)



(b)

Figure 3. The complete set of analyzed corrosion test data: (a) the measured oxide thickness, and (b) in the non-dimensionalized form that all collapsed onto one universal curve based on the oxidation and corrosion kinetic model.

Bibliography

The references for the reported data are in the attached database. Below is a list of the modeling and analysis paper the LANL team published or submitted over the years.

1. J. Zhang, N. Li, "Analysis of Liquid Metal Corrosion-Oxidation Interactions", submitted to **Corrosion Science** (2006).
2. J. Zhang, N. Li, "Comparisons of the Oxide Layer Between Static Liquid Lead-Bismuth Eutectic and Gas Environments", in **Proceedings of 14th International Conference on Nuclear Engineering** (ICONE14), Miami, US (2006).
3. N. Li, J. Zhang, B.H. Sencer, D. Koury, Surface Treatment and History-Dependent Corrosion in Lead-Alloy Systems, **Nuclear Instrumentation and Methods** (2006).
4. M. Machut, K. Sridharan, N. Li, T. Allen, "Corrosion Performance of Surface Modified Materials for Lead-Cooled Reactors", accepted for publication in **Journal of Nuclear Materials** (2006).
5. J. Zhang, N. Li, Y. Cheng, Dynamics of High Temperature Oxidation Accompanied by Scale Removal and Implications for Technological Applications, **Journal of Nuclear Materials**, (2005).
6. J. Zhang, N. Li, Oxidation Mechanisms of Steels in Liquid Lead-Alloys, **Oxidation of Metals**, 2005, 63 (5/6).
7. J. Zhang, N. Li, A. E. Russanov, Corrosion Behaviors of US Steels in Flowing Lead-Bismuth Eutectic (LBE), **Journal of Nuclear Materials**, 2005, 336, 1-10.
8. J. Zhang, N. Li, Corrosion/precipitation in non-isothermal and multi-Modular LBE Loop, **Journal of Nuclear Materials**, 2004, 326, 201-210.
9. J. Zhang, N. Li, Analytical Solution on Transient Corrosion/Precipitation in Closed Loop Systems, **Corrosion**, 2004, 60(4). 331-341.
10. J. Zhang, N. Li, A Correlation of Steel Corrosion in Non-isothermal LBE Loop Systems, **Journal of Nuclear Science and Technology**, 2004, 41(3). 260-264.
11. J. Zhang, N. Li, Parametric Study of a Corrosion Model Applied to Lead-Bismuth Flow Systems, **Journal of Nuclear Materials**, 2003, 321, 184-191.
12. J. Zhang, N. Li, Improved Application of Local Models to Steel Corrosion in Lead-Bismuth loops, **Nuclear Technology**, 2003, 142, 379-387.

13. N. Li, "Active Control of Oxygen in Molten Lead-Bismuth Eutectic Systems to Prevent Steel Corrosion and Coolant Contamination", **Journal of Nuclear Materials**, 300 (2002) 73-81.
14. X. Y. He, N. Li, and M. Mineev, "A Kinetic Model for Corrosion and Precipitation in Non-isothermal LBE Flow Loop", **Journal of Nuclear Materials**, 297 (2001) 214-219.

Attachment

Pb/LBE Corrosion Database 2006 (CD-ROM, to be delivered separately).